HIGH-TEMPERATURE OXIDATION OF FOUR HOT-WORK TOOL STEELS

VISOKOTEMPERATURNA OKSIDACIJA ŠTIRIH ORODNIH JEKEL ZA DELO V VROČEM

Tilen Balaško[1], Jaka Burja[2], Jožef Medved[1]

[1]University of Ljubljana, Faculty of Natural Sciences and Engineering, Aškerčeva cesta 12, 1000 Ljubljana, Slovenia
[2]Institute of Metals and Technology, Lepi pot 11, 1000 Ljubljana, Slovenia
tilen.balasko@omm.ntf.uni-lj.si

Hot-work tool steels have very good mechanical properties, especially strength, hardness and wear resistance at high temperatures. Therefore, hot-work tool steels are used for different applications, such as the high-pressure die casting of light alloys, the extrusion of polymers and forging. Since all these processes are operating at high temperatures, the main focus of this research was to investigate the high-temperature oxidation resistance of tool steels. We investigated the high-temperature oxidation at two different temperatures: 500 °C and 700 °C. The following tool steels were analyzed: HTCS-130, W600, RavnexHD and Dievar. Tests were made in an air atmosphere, while the heating and cooling were made in a controlled argon atmosphere. Simultaneous thermal analysis (STA 449 C Jupiter), scanning electron microscopy (SEM and EDS) and X-ray diffraction were used as the investigation methods. The results showed that during high-temperature oxidation at 500 °C Dievar steel has the best oxidation resistance, followed by RavnexHD, HTCS-130 and W600. However, at 700 °C the results were different, HTCS-130 had the best oxidation resistance, followed by Dievar, W600 and RavnexHD.

Keywords: tool steels, oxidation, simultaneous thermal analysis (STA), X-ray diffraction (XRD)

Orodna jekla za delo v vročem imajo zelo dobre mehanske lastnosti, med katerimi so najpomembnejše trdnost, trdota in obrabna obstojnost pri visokih temperaturah. Uporabna so predvsem za izdelavo orodij za tlačno litje lahkih kovin, ekstruzijo polimerov in utopno kovanje. Ker vsi ti procesi potekajo pri visokih temperaturah, je bil namen raziskave ugotavljanje korozijske obstojnosti preiskovanih jekel pri visokih temperaturah. Visokotemperaturno oksidacijo smo preiskovali pri dveh temperaturah: 500 °C in 700 °C. Analizirali smo naslednja orodna jekla: HTCS-130, W600, RavnexHD in Dievar. Preizkusi so potekali v kontrolirani atmosferi zraka, medtem ko sta segrevanje in ohlajanje potekala v zaščitni atmosferi argona. Uporabili smo napravo za simultano termično analizo (STA 449 C Jupiter), nato pa smo vzorce analizirali še s pomočjo vrstične elektronske mikroskopije (SEM in EDS), ter rentgenske difrakcije (XRD). Rezultati so pokazali, da je pri temperaturi oksidacije 500 °C korozijsko najbolj obstojno jeklo Dievar, sledijo RavnexHD, HTCS-130 in W600. Pri temperaturi oksidacije 700 °C pa je korozijsko najbolj obstojno jeklo HTCS-130, sledijo Dievar, W600 in RavnexHD.

Ključne besede: orodna jekla, oksidacija, simultana termična analiza (STA), rentgenska difrakcija (XRD)

1 INTRODUCTION

Hot-work tool steels are commonly used for high-pressure, die-casting molds. With every casting cycle, the mold is heated up and then cooled down, which means the surface begins to slowly oxidize.[1] Since these steels are used at high temperatures, we decided to study the influence of the different chemical compositions of the investigated steels on the high-temperature oxidation. The main reason for the research of this topic is the scarcity of similar investigations. Understanding the nature of oxidation is very important for a die life-span evaluation.

The high-temperature oxidation of iron is stable under isothermal conditions for long periods of time and usually follows the parabolic rate law.[2] Oxidation between 700 °C and 1250 °C follows the parabolic-oxidation regime and develops three layers: an outermost thin hematite layer (Fe_2O_3), a thin intermediate magnetite layer (Fe_3O_4), and a thick inner wüstite layer (FeO).[3] The thickness of every layer reflects the diffusion rate of the

Fe in it. The Fe diffusion in wüstite is much greater than in hematite and magnetite.[4] On the other hand, the high-temperature oxidation of steels is much more complex. The main reason is the presence of impurities and alloying elements in the steels that affect the oxidation process.[2] The oxidation rate grows with the temperature, and at 570 °C the oxidation becomes very rapid. Above that temperature, we should have three oxide layers: FeO, Fe_3O_4 and Fe_2O_3. FeO is thermodynamically unstable under 570 °C.[5]

The influence of alloying elements on the kinetics of the high-temperature oxidation of hot-work tool steels should be considered. Molybdenum can improve the oxidation of steel up to 900 °C for 10 h, but it has a catastrophic influence after 10 h and above 900 °C.[6] High Mo steels are prone to segregations and the formation of intermetallic phases such as σ, γ and Laves phases above 900 °C, which lower the oxidation resistance and make them vulnerable to cracking during hot working.[6–9] Steels with higher Mo content typically face

Table 1: Chemical composition for the investigated steels in mass fractions

Steel	Chemical elements											
	C	Si	Mn	P	S	Cr	Ni	V	W	Cu	Mo	Fe
HTCS-130	0.31	0.07	0.08	0.007	0.001	0.1	0.04	0.01	1.9	0.04	3.2	Bal.
RavnexHD	0.36	0.30	0.40	< 0.01	0.001	5.00	1.65	0.60	<0.01	<0.01	1.70	Bal.
W600	0.32	0.12	0.23	0.005	0.001	0.11	2.1	<0.01	1.9	0.01	3.2	Bal.
Dievar	0.34	0.17	0.44	0.008	0.001	5.05	0.19	0.54	0.01	0.08	2.37	Bal.

oxidation complications above 900 °C due to MoO_3 formation.[10–12] Since we studied oxidation below 900 °C the Mo should improve the oxidation resistance.

The addition of Ni improves the high-temperature oxidation resistance of low-carbon high-strength steels.[13–16] Fukugawa et al. indicate that Ni reduces the oxidation rate and promotes inner oxidation.[13] Meanwhile, Si degrades the high-temperature oxidation resistance of steels with low amounts of Cu and Ni.[13,17] Silicon promotes inner oxidation and the formation of low-temperature-melting fayalite $(2FeO.SiO_2)$.[13,18,19] Chromium is a well-known alloying element that increases resistance to high-temperature oxidation. There is a critical Cr concentration (~12 $w/\%$) for the formation of a protective Cr_2O_3 surface layer.[20] Small amounts of Mn can lower the critical Cr concentration. A thin compact oxide layer forms, mostly composed of Mn-Cr spinels and Cr-rich oxides, which improve the high-temperature oxidation resistance. Therefore, Mn indirectly increases the high-temperature oxidation resistance.[20]

2 EXPERIMENTAL PART

Four hot-work tool steels were investigated. The chemical compositions of the investigated steels are shown in **Table 1**. Samples with a diameter of 4 mm and a height of 1.75 mm were used with thermogravimetric analyses (TG). Because the results of the high-temperature oxidation are usually given in mass change after a certain time per specific surface of the sample examined the samples were grinded to a smooth surface. The thermogravimetric analysis was made in NETZSCH STA 449 C Jupiter thermal analyzer. The samples were heated at 20 K/min in a protective Ar atmosphere to the oxidation temperature, and then an air atmosphere was
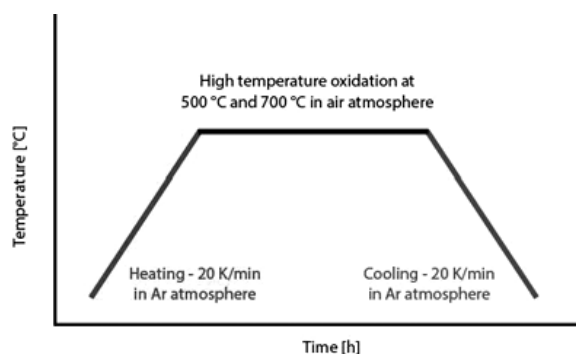
Figure 1: Schematic presentation of the oxidation process

introduced. The samples were held at the temperature for 48 h. The cooling was carried out in an argon atmosphere at 20 K/min to room temperature. The oxidation was carried out at two different temperatures, i.e., 500 °C and 700 °C. A schematic presentation of the oxidation process is shown in **Figure 1**.

After the oxidation the samples were metallographically prepared for scanning electron microscopy (SEM). We measured the thickness of the oxide layer for all the experimental samples with the SEM (JEOL JSM-5610). We also used EDS (Energy-dispersive X-ray spectroscopy) analysis to determine the composition of the oxide layer.

For the X-ray diffraction (XRD) studies larger samples (20 mm × 40 mm × 10 mm) were put into annealing furnaces heated to 500 °C and 700 °C, and held at temperature for 48 h in an air atmosphere. We used a PANalytical 3040 X-ray Diffractometer for XRD analysis.

3 RESULTS AND DISCUSSION

3.1 Thermogravimetry (TG)

We investigated the mass change of the steel samples at the two different temperatures. The results of the thermogravimetric analyses for high-temperature oxidation at 500 °C are shown in **Figure 2** and **Table 2**. W600 gained the most weight, i.e., 1.91 mg/cm², which means it is the least resistant to high-temperature oxidation at 500 °C. The second was HTCS-130, which gained 1.55 mg/cm². RavnexHD was third, the mass gain was 1.33 mg/cm². The most oxidation-resistant steel at 500 °C was Dievar, with a mass change of 0.96 mg/cm². The parabolic law can describe all the oxidation rates of the investigated steels, and some parts are even linear (**Figure 2**). The reason why Dievar and RavnexHD are the most resistant to oxidation at 500 °C is the Cr content (5 $w/\%$). Chromium starts to form a protective Cr_2O_3 layer during high-temperature oxidation.[21] Dievar has better resistance than RavnexHD, because of the higher Mo and the lower Ni and Si contents.

The results of the high-temperature oxidation at 700 °C are presented in **Figure 3**. The higher temperature and consequently higher diffusion rates of the elements give different results, as presented in **Table 2**. RavnexHD gained the most weight (15.65 mg/cm²), second was W600 (13.82 mg/cm²), third was Dievar (9.33 mg/cm²), while the most oxidation-resistant steel at
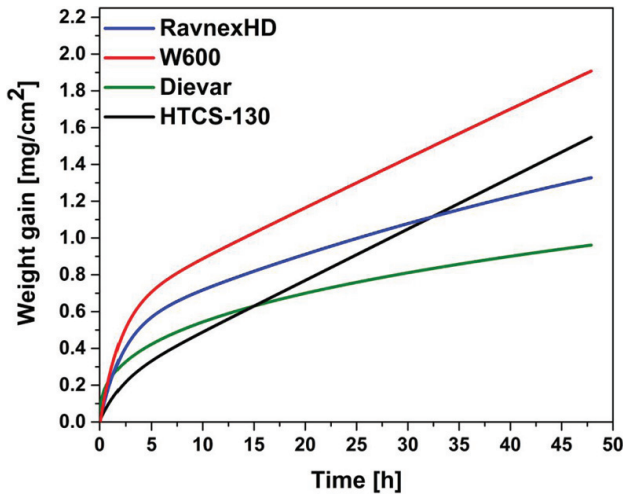
Figure 2: Mass change per specific surface depending on the time at 500 °C

700 °C was HTCS-130, with a mass change of 2.45 mg/cm². The main reason is the ratio between the chemical elements. HTCS-130 has the lowest amount of C, Si, Cr, Ni and Mn, compared to the other investigated steels (**Table 1**). While the second steel, Dievar has high Mo, Cr, Mn and V content. The first three chemical elements give Dievar high-temperature oxidation resistance. Meanwhile, W600 and RavnexHD have the highest mass change; the reason is the combination of Ni and Mo (high Ni and Mo cause porous scale formation).[22]
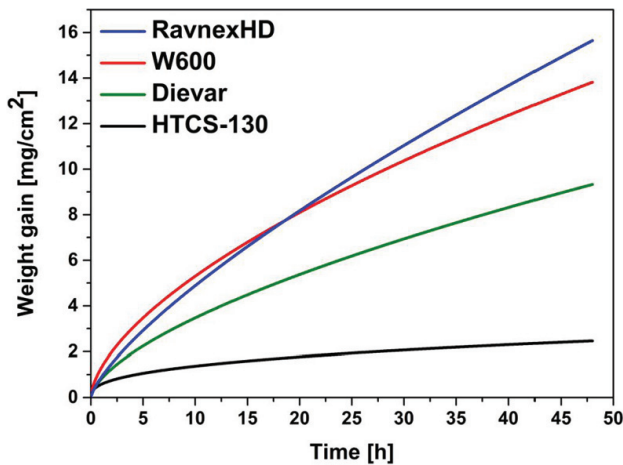
Figure 3: Mass change per specific surface depending on the time at 700 °C

Table 2: Change in mass for investigated steels at investigated temperatures

Steel	Average change in mass at temperature of 500 °C (mg/cm²)	Average change in mass at temperature of 700 °C (mg/cm²)
HTCS-130	1.55	2.45
W600	1.91	13.82
RavnexHD	1.33	15.65
Dievar	0.96	9.33
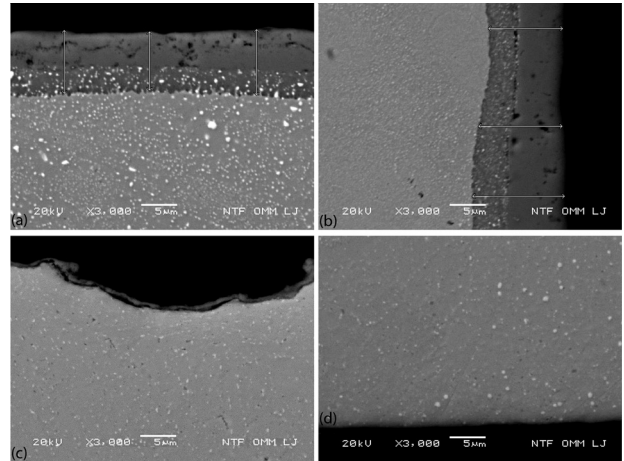
Figure 4: Thickness of the oxide layer at 500 °C of: a) HTCS-130, b) W600, c) RavnexHD and d) Dievar

RavnexHD has a lower oxidation resistance at 700 °C compared to W600, due to the lower Mo content.

3.2 Scanning electron microscopy (SEM)

The TG samples' oxide layers were analyzed with SEM. First, we measured the thickness of the oxide layers, as shown in **Figure 4** and **5**. At 500 °C, we can clearly see that the oxide layer consists of two oxide layers (**Figure 4a** and **4b**). The inner layer still contains carbides in the case of HTCS-130 and W600; these are Mo and W carbides (M6C, M2C and MC). The outer layer is porous (**Figure 4a** and **4b**). As we can see, **Figure 4c** (RavnexHD), has a thin oxide layer that is barely visible, while Dievar has no visible oxide layer and could not be measured (**Figure 4d**).

The oxide layers that formed during oxidation at 700 °C are visible in **Figure 5**. The oxide layers formed at 700 °C are thicker than at 500 °C, as expected from the TG results. The average thicknesses of the oxide layers are presented in **Table 3**. The structure of the
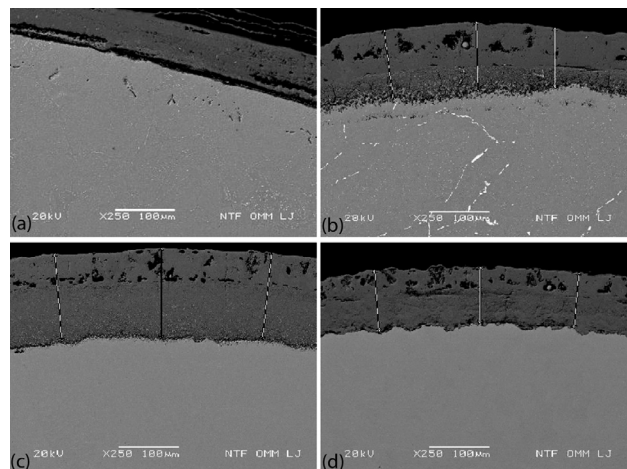
Figure 5: Thickness of the oxide layer at 700 °C of a) HTCS-130, b) W600, c) RavnexHD and d) Dievar

samples' oxide layers at 700 °C is almost the same as at 500 °C. The only difference is the thickness, i.e., the oxide layer is thicker at 700 °C. The outer layer gets more porous at 700 °C (**Figure 5**).

There are two oxide layers, which is most evident in **Figure 5b**. The inner oxide layer still has some undissolved carbides. However, there are fewer carbides in the inner oxide layer at 700 °C than at 500 °C.

Table 3: Average thickness of oxide layer for all investigated steels

Steel	Average thickness of the oxide layer at 500 °C (µm)	Average thickness of the oxide layer at 700 °C (µm)
HTCS-130	8.01	26.3
W600	10.68	120.0
RavnexHD	0.53	144.0
Dievar	/	97.0

We analyzed the chemical composition of the oxide layers with EDS. The results show that the outer layer in all the analyzed samples consists of iron and oxygen at 500 °C, while at 700 °C we also noticed some other chemical elements. These are alloying elements with the highest w/% in steels. Mo and W were found in the HTCS-130 and W600 outer oxide layer. Dievar and RavnexHD also have some Mn in the outer layer at 700 °C; this is consistent with $MnO.Cr_2O_3$ formation.[23] On the other hand, the inner layers were slightly more complex; they contained more alloying elements than the outer layers (**Table 4** and **Table 5**). In the case of HTCS-130 and W600 (at 500 °C and 700 °C) Mo and W were detected; however, in the oxide layer of W600 we also detected some Ni. On the other hand, in the inner oxide layer of RavnexHD we detected Cr, Mo, V, Ni, Si, and Mn. Dievar had Cr, Mo, V, Si and Mn in the inner oxide layer. This was expected, because those are the main alloying elements. The results of the EDS analyses of the Dievar steel at 500 °C are not presented (**Table 4**), because there was no oxide layer to analyze.

Table 4: EDS results of the inner oxide layer of the investigated steels after high-temperature oxidation at 500 °C in mass fractions

Steel	Chemical elements								
	O	Fe	Mo	W	Ni	Si	V	Cr	Mn
HTCS-130	3.10	86.71	6.52	3.67	/	/	/	/	/
W600	3.42	89.80	3.84	2.38	0.56	/	/	/	/
RavnexHD	3.90	85.91	1.51	/	0.99	0.47	1.30	5.54	0.38

Table 5: EDS results of inner oxide layer of investigated steels after high temperature oxidation at 700 °C in mass fractions

Steel	Chemical elements								
	O	Fe	Mo	W	Ni	Si	V	Cr	Mn
HTCS-130	3.98	74.35	16.91	4.60	/	/	/	0.16	/
W600	4.035	84.575	6.35	3.99	0.69	/	/	0.21	0.15
RavnexHD	2.605	85.585	2.32	/	1.92	0.47	0.73	6.14	0.23
Dievar	2.79	89.23	2.12	/	/	0.31	0.53	4.81	0.21

3.3 X-ray diffraction results

The oxide scales formed on the investigated hot-work tool steels were analyzed by XRD. At 500 °C Dievar has the thinnest oxide layer (**Table 3**), which is why the diffraction peak of the matrix (α_{Fe}) is the most intensive (**Figure 6**). RavnexHD has a less intense diffraction peak of the matrix than Dievar (**Figure 6**), because it has a thicker oxide layer. W600 has a relatively thick oxide layer, so the matrix (α_{Fe}) diffraction peak is even less intensive (**Figure 6**). The diffraction-peak intensities are consistent with the temperature of the high-temperature oxidation. HTCS-130 has a similar trend to W600:
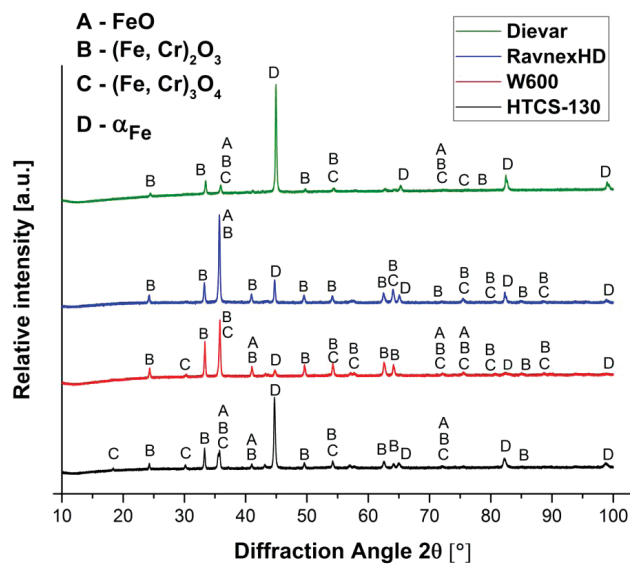
Figure 6: XRD patterns of the samples after oxidation at 500 °C
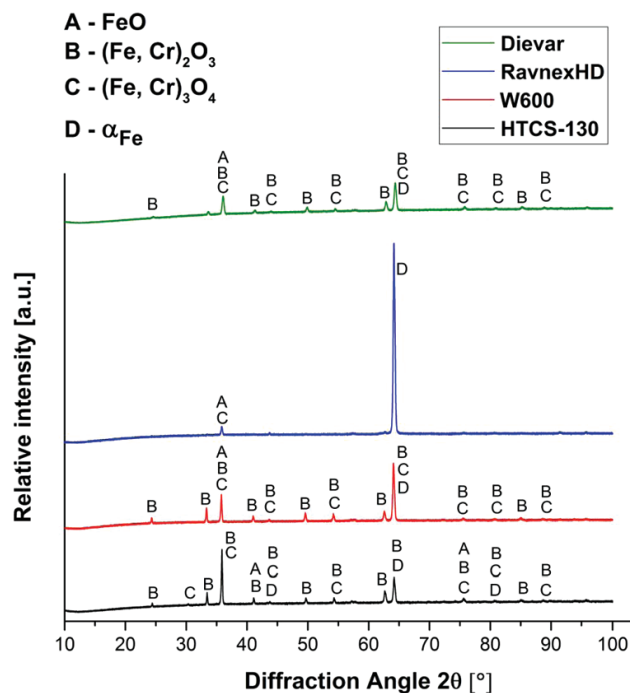
Figure 7: XRD patterns of the samples after oxidation at 700 °C

hematite dominates, followed by magnetite and wüstite (**Figure 6**). Hematite (Fe_2O_3 – B in **Figure 6**) predominates, but we also notice some magnetite (Fe_3O_4 – C in **Figure 6**), and there are also beginnings of wüstite (FeO – A in **Figure 6**) formation in Ravnex HD and Dievar.

At higher temperatures, 700 °C (**Figure 7**), we are closer to establishing the thermodynamic equilibrium of wüstite; more FeO (A in **Figure 7**) is present at elevated temperatures. HTCS-130 still has a lot of hematite (**Figure 7**), followed up by magnetite and wüstite. On the other hand, Dievar has less magnetite, hematite and almost no wüstite (**Figure 7**). W600 has also very little wüstite, hematite is still dominating, followed by magnetite (**Figure 7**). In comparison to other samples, RavnexHD has the thickest oxide layer, but the XRD result shows only magnetite and wüstite in the oxide layer (**Figure 7**).

If we compare the results at 500 °C and 700 °C, we notice that there are a few changes in the oxide types, because the stabilities of the oxide phases (FeO, Fe_2O_3 and Fe_3O_4) are functions of the oxidation temperature and the ambient oxygen partial pressure. Wüstite should be stable above 570 °C in air; however, it has been found in thin films down to 400 °C.[23] In our case we found wüstite at 500 °C (**Figure 6**). There is a strong relationship between the Fe (in our case hot-work tool steel) surface and the composition and thickness of the initial oxide. The first oxide that starts to form consists of Fe_2O_3 and Fe_3O_4, growth follows the parabolic kinetics, where the rate is dominated by the diffusional transport of Fe^{2+} and Fe^{3+} ions through the oxide grain boundaries. At temperatures below 500 °C the Fe_3O_4 nucleates first, followed up by Fe_2O_3, which nucleates on the Fe_3O_4. In addition, the oxidation of iron/steel often shows an unusual dependence on the oxygen pressure.[23] These are the reasons why we have mostly hematite (Fe_2O_3) and magnetite (Fe_3O_4) in our investigate oxide layers (**Figure 6** and **Figure 7**).

4 CONCLUSIONS

The following conclusions can be drawn from the paper. At 500 °C Dievar was the most oxidation-resistant steel, followed by RavnexHD, HTCS-130 and W600. The reason for the good high-temperature oxidation resistance of Dievar and RavnexHD is the high Cr content; it forms a protective Cr_2O_3 layer. At 700 °C HTCS-130 was the most oxidation-resistant steel, followed by Dievar, W600 and RavnexHD. The main reason for the very good oxidation resistance of HTCS-130 in comparison to the other steels is the ratio between the alloying elements and the high content of Mo, which improves the oxidation resistance. W600 has almost the same chemical composition as HTCS-130, but it seems that higher contents of Ni, Si and Mn decrease the oxidation resistance in this case.

5 REFERENCES

[1] G. Roberts, G. Krauss, R. Kennedy, Tool Steels, 5th ed., ASM, Ohio USA 1998, 364
[2] R. Y. Chen, W. Y. D. Yuen, Review of the high-temperature oxidation of iron and carbon steels in air or oxygen, Oxidation of Metals, 59 (**2003**) 5-6, 433–468, doi:10.1023/A:1023685905159
[3] M. H. Davies, M. T. Simnad, C. E. Birchenall, On the mechanism and kinetics of the scaling of iron, C.E. JOM, 3 (**1951**), 889–896, doi:10.1007/BF03397397
[4] J. B. Newkirk, High-temperature materials coatings and surface interactions, Freund Publishing House, Israel 1980, 314
[5] L. Vehovar, Korozija kovin in korozijsko preskušanje, Ljubljana 1991, 48
[6] L. Huabing, Z. Binbin, J. Zhouhua, Z. Shucai, F. Hao, H. Peide, D. Nan, Z. Wei, L. Guoping, F. Guangwei, L. Qizeng, A new insight into high-temperature oxidation mechanism of super-austenitic stainless steel S32654 in air, Journal of Alloys and Compounds, 686 (**2016**), 326–338, doi:10.1016/j.jallcom.2016.06.023
[7] S. Heino, B. Karlsson, Cyclic deformation and fatigue behaviour of 7Mo-0.5N superaustenitic stainless steel-stress-strain relations and fatigue life, Acta Materialia, 49 (**2001**) 2, 339–351, doi:10.1016/S1359-6454(00)00200-7
[8] E. X. Pu, W. J. Zhang, J. Z. Xiang, Z. G. Song, J. Li, Hot deformation characteristic and processing map of superaustenitic stainless steel S32654, Material Science and Engineering: A, 598 (**2014**), 174–182, doi:10.1016/j.msea.2014.01.027
[9] G. V. Prasad Reddy, R. Sandhya, S. Sankaran, P. Parameswaran, K. Laha, Creep-fatigue interaction behavior of 316LN austenitic stainless steel with varying nitrogen content, Materials & Design, 88 (**2015**), 972–982, doi:10.1016/j.matdes.2015.09.007
[10] F. J. Perez, E. Otero, M. P. Hierro, C. Gomez, F. Pedraza, J. L. de Segovia, E. Roman, High temperature corrosion protection of austenitic AISI 304 stainless steel by Si, Mo and Ce ion implantation, Surface and Coatings Technology, (**1998**) 108–109, 127–131, doi:10.1016/S0257-8972(98)00685-9
[11] V. Behrani, A. J. Thom, M. J. Kramer, M. Akinc, Microstructure and oxidation behavior of Nb-Mo-Si-B alloys, Intermetallics, 14 (**2006**) 1, 24–32, doi:10.1016/j.intermet.2005.03.007
[12] P. K. Ray, M. Akinc, M. J. Kramer, Formation of multilayered scale during the oxidation of NiAl-Mo alloy, Applied Surface Science, 301 (**2014**), 107–111, doi:10.1016/j.apsusc.2014.01.148
[13] Y. Liu, C. Yang, F. Chai, T. Pan, H. Su, High temperature oxidation resistance of 9Ni steel, Journal of iron and steel research, International, 21 (**2014**) 10, 956–963, doi:10.1016/S1006-706X(14)60168-0
[14] C. K. Syn, B. Fultz, J. W. Morris, Jr., Mechanical stability of retained austenite in tempered 9Ni steel, Metallurgical and Materials Transactions A, 9 (**1978**) 11, 1635–1640, doi:10.1007/ BF02661946
[15] J. R. Strife, D. E. Passoja, The effect of heat treatment on microstructure and cryogenic fracture properties in 5Ni and 9Ni steel, Metallurgical Transactions A, 11 (**1980**) 8, 1341–1350, doi:10.1007/BF02653488
[16] B. Fultz, J. I. Kim, Y. H. Kim, H. J. Kim, G. O. Fior, J. W. Morris, The stability of precipitated austenite and the toughness of 9Ni steel, Metallurgical Transactions A, 16 (**1985**) 12, 2237–2249, doi:10.1007/BF02670423

[17] T. Fukagawa, H. Okada, Y. Maegara, Mechanism of red scale defects formation in Si-added hot-rolled steel sheets, ISIJ International, 34 (**1994**) 11, 906–911, doi:10.2355/isijinternational.34.906

[18] L. Yin, S. Balaji, S. Sridhar, Effects of nickel on the oxide/metal interface morphology and oxidation rate during high-temperature oxidation of Fe–Cu–Ni alloys, Metallurgical and Materials Transactions B, 41 (**2010**) 3, 598–611, doi:10.1007/s11663-009-9334-z

[19] E. J. Song, D. W. Suh, H. K. D. H. Bhadeshia, Oxidation of silicon containing steel, Ironmaking & Steelmaking, 39 (**2012**) 8, 599–604, doi:10.1179/1743281212Y.0000000007

[20] X. Jin, S. Chen, L. Rong, Effects of Mn on the mechanical properties and high temperature oxidation of 9Cr2WVTa steel, Journal of Nuclear Materials, 494 (**2017**), 103–113, doi:10.1016/j.jnucmat. 2017.07.024.

[21] A. Col, V. Parry, C. Pascal, Oxidation of a Fe–18Cr–8Ni austenitic stainless steel at 850 °C in O2: Microstructure evolution during breakaway oxidation, Corrosion Science, 114 (**2017**), 17–27, doi:10.1016/j.corsci.2016.10.029

[22] S. S. Brenner, Oxidation of iron-molybdenum and nickel-molybdenum alloys, Journal of The Electrochemical Society, 102 (**1955**) 1, 7–15, doi:10.1149/1.2429990

[23] T. Richardson, Shreir's Corrosion, 1st ed., Elsevier Science, 2009, 4000